university of groningen

faculty of science and engineering

Feasibility study of a search for lepton-flavour violating $\Lambda_b \to \Lambda\mu\tau$ decays at the LHCb experiment

Author:
Ignacio Jacob UROZ RODRÍGUEZ
(s5118913)

Supervisor:
dr. Ann-Kathrin PERREVOORT
Second examiner :
prof. Julia EVEN

Bachelor's Thesis
To fulfill the requirements for the degree of
Bachelor of Science in Physics
at the University of Groningen

July 18, 2025

Contents

Abstract

Abstract

This research project presents a feasibility study of the search for the lepton-flavour violating (LFV) decay $\Lambda_b^0 \to \Lambda^0 \mu^- \tau^+$ using simulations made in RapidSim. The analysis explores which key observables, particularly the invariant mass and the corrected mass, allow for effective discrimination between signal and the potential background process $\Lambda_b^0 \to \Lambda^0 \tau^- \tau^+$.

Distributions for the invariant mass and corrected mass of the reconstructed Λ_b^0 candidates were generated and compared. The corrected mass was found to significantly improve the resolution and alignment with the true Λ_b^0 mass, particularly in signal events with a single undetected neutrino in its final state. In contrast, the background events, which include three neutrinos in the final state, exhibited a broader and more shifted distribution. This leads to a clear separation between signal and background, with the corrected mass emerging as the most promising variable for future searches of LFV decays.

While the results are promising, the study is based on fast simulation and does not include full detector effects, efficiencies, or systematic uncertainties. Future work should incorporate full Monte Carlo simulations within the LHCb framework to validate and extend these findings. Nevertheless, this study demonstrates that the corrected mass can provide a powerful tool in the search for rare LFV processes in baryonic decays.

Acknowledgments

I want to deeply thank my supervisor Ann-Kathrin Perrevoort for guiding me through these months. I have felt the most fortunate student ever since I knew that she would be supervising my thesis, due to the fact that Subatomic Physics is the field that I love the most among all Physics. Furthermore, I want to thank the LHCb Groningen team, since everyone helped me to solve any small doubt I had and always with a smile in their faces. It has been a true pleasure to do this beautiful research with such talented and caring people working side by side with me.

1 Introduction

Symmetries are a very significant element in the field of Subatomic Physics [1], since they are determinant when studying the fundamental forces of the universe. Usually, charge conjugation C, parity inversion P and time reversal T are the main symmetries considered in physics processes [2], there are other symmetries, such as conservation laws that are expected to be preserved.

In order to describe and understand the fundamental particles and their interactions (excluding gravity) that compose the Universe, the Standard Model of particle physics (SM) is taken into consideration [3]. This model successfully unifies the electromagnetic, weak, and strong interactions, predicting the existence of particles such as the Higgs boson, which was confirmed in 2012 [4]. Within the SM, fermions are grouped into three generations, each containing a charged lepton, a neutrino, and two types of quarks. Leptons, which are of high interest in this research, are fermions with half integer spin and either integer or zero charge. The generations of leptons are also denominated flavours, and they are conserved according to the Standard Model. However, despite its predictive power, the Standard Model is known to be incomplete. It does not incorporate gravity, explain the neutrino masses, nor account for the asymmetry of dark matter or the matter–antimatter in the universe [5, 6]. Furthermore, all lepton flavour transitions involving charged leptons are highly suppressed or forbidden in the SM framework [7, 8]. This strong suppression is exemplified by the predicted branching ratio for the decay $\mu \to e\gamma$, which is of the order of 10^{-54} within the SM extended by neutrino masses [9]. This makes such processes effectively unobservable in the absence of New Physics.

Lepton Flavour Violation, usually shortened as LFV, is the name that describes subatomic processes in which the total lepton number L is conserved, but the lepton numbers from each lepton flavour, that is L_e, L_μ and L_τ are not conserved [10]. The discussion about whether lepton flavour was a conserved quantity in nature or not has already been proved with the results from observations of neutrino oscillations. These oscillations, confirmed theoretically and experimentally in the late 20th century in experiments such as the Super-Kamiokande [11], were the basis to explain that neutrino flavour could change between the three generations of leptons, which are electron, muon and tau [12]. Thus, neutrino flavour eigenstates were interpreted as a superposition mass eigenstates, demonstrating that neutrinos have non-zero mass and violate lepton flavour. When neutrinos travel through space, the superposition evolves and leads to transitions between the three lepton flavours.

Naturally, if neutrinos proved the fact that lepton flavour was not a symmetry in nature, it is a must to investigate whether LFV also apply to processes where charged leptons are involved - Charged Lepton Flavour Violation, shortened as CLFV. Due to the fact that in the Standard Model, processes are expected to conserve the lepton flavour number when charged leptons are involved, CLFV leads to what is known as Physics beyond the Standard Model [13]. In the SM, lepton flavour is conserved, being this fundamental to understand why those processes where charged lepton flavour is violated are suppressed to negligible levels (branching ratios $\sim 10^{-54}$) due to the GIM mechanism and the smallness of neutrino masses [14]. Therefore, any observable CLFV would constitute a clear signature of Physics beyond the SM (BSM), making it a powerful probe for new theories such as leptoquarks, heavy neutral leptons, or extended Higgs sectors [13]. There are many processes that have been studied in order to search for New Physics. The most stringent constraints to date arise from muon-based experiments. The MEG collaboration has set a remarkable upper limit on the branching ratio of the decay $\mu^+ \to e^+\gamma$ at 4.2×10^{-13} [9]. Tau decays also provide a rich laboratory for CLFV, as the heavier mass of the τ lepton allows for a wider range of decay modes. Experiments such as Belle have aimed for processes like $\tau \to \mu\gamma$, $\tau \to 3\mu$, and $\tau \to \mu\eta$, placing upper limits on the order of 10^{-8} for many decay channels [15]. Interestingly, even flavour-conserving transitions such as $b \to s\ell^+\ell^-$, allowed within the Standard Model, have shown anomalies in relation with theoretical

predictions. There are discrepancies in angular observables (such as P_5' in $B^0 \to K^{*0}\mu^+\mu^-$). These anomalies have sparked significant theoretical interest, with many models proposing the existence of new mediators such as leptoquarks or Z' bosons to explain the data [16, 17]. As such, the study of lepton flavour violation in processes like $\Lambda_b^0 \to \Lambda^0\mu^\mp\tau^\pm$ becomes even more compelling in the context of this broader set of tensions between experiment and the Standard Model. B^0 meson decay to K^{*0} meson, $\tau^\pm$ lepton and $\mu^\mp$ lepton [18]. It is of high interest to notice that CLFV originates from the a decay channel of the beauty quark that has the following form: $b \to s\ell^+\ell^-$. This means that the beauty quark decays to a strange quark and two leptons with different charge. Since these two leptons can be of different flavour, that is where CFLV occurs. This is because the lepton flavour number of any of the leptons is zero on the left side, where there is only a beauty quark. However the lepton flavour number is non zero on the right side, since a tau and muon are produced.

For this research, the objective is to search for CFLV in the decay $\Lambda_b^0 \to \Lambda^0\mu^\mp\tau^\pm$, simulated by using proton-proton collision data from the LHCb experiment. This baryon decay, where the charged lepton flavour is not conserved has not been attempted before. Taking into consideration the fact that the quark content of the Λ_b baryon is *udb* and the quark content of the Λ_0 baryon is *uds* [19], it can be seen that the lepton flavour number is violated due to obtaining a tau and a muon as decay products from the beauty quark decay $b \to s\ell^+\ell^-$. Therefore, by studying the kinematics and differ the signal decays from the background processes, it will be known how feasible is to search for this lepton flavour violating decay. In brief, this research project contributes to look for Physics beyond the Standard Model, investigating whether the LHCb detector has the sensitivity required to observe or constrain such a rare decay, and thereby provide further insight into the nature of lepton flavour conservation.

1.1 Research Questions

To summarize, this research project aims to answer the following question:

Q1. How feasible is it to search for charged lepton flavour violation in the decay $\Lambda_b^0 \to \Lambda^0\mu^\mp\tau^\pm$ at the LHCb experiment?

Q2. Which kinematic variables are most effective in distinguishing signal decays from background processes in this channel?

1.2 Thesis Outline

This thesis is structured to provide a comprehensive overview of the theoretical, experimental, and analytical aspects involved in assessing the feasibility of observing lepton flavour violation in the decay $\Lambda_b^0 \to \Lambda^0\mu^\mp\tau^\pm$. The work begins with an introduction to the relevance of symmetries in particle physics, followed by a conceptual foundation on lepton flavour violation, neutrino oscillations, and charged lepton flavour violation (CLFV), highlighting why such processes are forbidden or heavily suppressed within the Standard Model. In the chapter on Background Literature, the theoretical underpinnings are explored more deeply, particularly focusing on the Glashow–Iliopoulos–Maiani (GIM) mechanism, the structure of flavour-changing neutral currents (FCNC), and the role of neutrino masses and mixing. This includes a discussion on how extensions beyond the Standard Model can give rise to CLFV processes at observable rates, motivating experimental searches in b-hadron decays.

Following the theoretical framework, the thesis presents an overview of the LHCb experiment, where the simulated data is assumed to originate. The detector components, triggering mechanisms, and particle identification strategies relevant to reconstructing Λ_b decays are discussed. Then, the

methodology chapter explains the simulation and reconstruction of the signal and background decays, using Monte Carlo tools such as RapidSim and ROOT. The selection of discriminating variables, including invariant masses, corrected mass, and vertex fit qualities, is described, together with the strategy for defining cuts that optimize signal-to-background separation.

The results chapter presents the analysis of these variables, showing how the signal can be distinguished from dominant background processes. The feasibility of the search is evaluated in terms of achievable sensitivity, possible background contamination, and the potential to place limits on the branching ratio of the decay. Finally, the thesis concludes with a summary of the findings and discusses the implications of the results in the broader context of flavour physics and searches for new Physics beyond the Standard Model.

2 Theoretical background

Lepton Flavour Violation is a widely discussed phenomenon in Physics, therefore it is important to take into account the different statements that have been made around this subject.

2.1 The Standard Model of Particle Physics

The Standard Model (SM) is the accepted theoretical paradigm that describes the fundamental particles of the universe and the interactions between them, excluding gravity [3]. It is based on quantum field theory and built upon the gauge symmetry group $SU(3)_C \times SU(2)_L \times U(1)_Y$, where each term represents one of the three fundamental forces it describes: the strong interaction, the weak interaction and the electromagnetic interaction, respectively.

The Standard Model shows that all matter is composed of elementary fermions, which are spin-$\frac{1}{2}$ particles. These are divided into two different categories: quarks and leptons. Quarks carry colour charge and therefore interact via the strong force, while leptons do not. Each category comes in three generations, also denominated flavours. For quarks, there is up (u), charm (c), and top (t) quarks with charge equal to $+\frac{2}{3}$, and down (d), strange (s), and bottom (b) quarks with charge equal to $-\frac{1}{3}$. Leptons are fermions that have either integer or zero charge. The generations of leptons include the electron (e), muon (μ), and tau (τ), each with a corresponding neutrino (ν_e, ν_μ, ν_τ). The fermion generations are distinguished by their masses. The higher the mass, the more unstable the fermion is.

The electromagnetic interaction is mediated by photons (γ), the weak interaction by the $W^\pm$ and Z^0 bosons, and the strong interaction by gluons (g). The Higgs boson (H), discovered in 2012 at the LHC [4], is responsible for giving mass to the W and Z bosons and to fermions through the Higgs mechanism, completing the Standard Model. The existence and discovery of the Higgs was a key milestone, since it conceded experimental confirmation of the mechanism of electroweak symmetry breaking.

Local gauge invariance is an important aspect of the Standard Model. Each interaction corresponds to a specific gauge symmetry: $SU(3)_C$ for quantum chromodynamics (QCD), $SU(2)_L$ for the weak isospin symmetry, and $U(1)_Y$ for hypercharge. Through the process of spontaneous symmetry breaking, the $SU(2)_L \times U(1)_Y$ group breaks down to $U(1)_{\mathrm{EM}}$, which gives rise to the electromagnetic interaction and confirms the fact that the photon is massless, since electromagnetic interaction has infinite range.

Nevertheless, the Standard Model does have limitations. It does not include gravity, and it does not explain certain phenomena such as the observed matter–antimatter asymmetry, dark matter, or dark energy. Furthermore, it does not incorporate neutrino masses in its minimal formulation — which is an issue, since neutrino oscillations have proven that neutrinos do in fact have mass, as it will be commented further on [5]. This already points to the necessity of extending the Standard Model, being a sign that it is not a conclusive model in physics, since there is phenomena beyond its boundaries.

2.2 Lepton Flavour Violation: From Neutrinos to Charged Leptons

Lepton flavour violation (LFV) is a concept that began to take form when neutrinos were found to change flavour as they traveled through space. These neutrino oscillations were experimentally confirmed in the late 20th century in key experiments such as Super-Kamiokande [11], which led to the conclusion that neutrinos have non-zero masses and that flavour is not a conserved quantity in the neutrino sector. This clearly violates the separate conservation of lepton numbers L_e, L_μ, and L_τ, but not the total lepton number $L = L_e + L_\mu + L_\tau$, which still holds. The value for L_ℓ is +1 in case of an

electron, electron neutrino, muon, muon neutrino, tau and tau neutrino, whereas L_ℓ is -1 in case of a positron, electron anti-neutrino, anti-muon, muon anti-neutrino, anti-tau and tau anti-neutrino.

The mechanism behind neutrino oscillations is modeled by the Pontecorvo – Maki – Nakagawa – Sakata (PMNS) matrix [20], which represents the mixing between the flavour eigenstates of the neutrinos and their mass eigenstates. This matrix is an unitary matrix that gives the likelihood for a neutrino originally produced with one of the three lepton flavours to be found with a different lepton flavour through their propagation. The matrix can be seen below, where ν_e is electron neutrino, ν_μ is muon neutrino and ν_τ is tau neutrino. The $U_{\alpha i}$ represent the mass amplitudes for each mass eigenstate $i = 1,2,3$ in terms of lepton flavour $\alpha = e,\mu,\tau$.

$$\begin{bmatrix} \nu_e \\ \nu_\mu \\ \nu_\tau \end{bmatrix} = \begin{bmatrix} U_{e1} & U_{e2} & U_{e3} \\ U_{\mu 1} & U_{\mu 2} & U_{\mu 3} \\ U_{\tau 1} & U_{\tau 2} & U_{\tau 3} \end{bmatrix} \begin{bmatrix} \nu_1 \\ \nu_2 \\ \nu_3 \end{bmatrix}$$

This mixing provides the foundation of lepton flavour violation in the Standard Model (SM), although it is considerably suppressed for charged leptons. Nevertheless, if lepton flavour is violated in the neutrino sector, it gives a clear clue already that this violation may happen also in the charged sector.

2.3 The GIM Mechanism

In the context of the SM, Charged Lepton Flavour Violation (CLFV) is technically allowed, but the possibility of finding it is very low. The suppression comes from what is called the Glashow – Iliopoulos – Maiani (GIM) mechanism [7], originally developed to explain the suppression of flavour-changing neutral currents (FCNC) in the quark sector. The GIM mechanism works through a cancellation that occurs when summing over internal quark generations in loop diagrams. The same principle can be extended to leptons, where the tiny neutrino masses ensure that the CLFV amplitudes cancel out almost completely.

For instance, in the decay $\mu \to e\gamma$, the loop diagram involves neutrinos. But since their masses are so tiny and the mixing angles are small, the decay rate ends up being $O(10^{-54})$ [8]. In the Standard Model, taking into consideration neutrino masses and mixing, charged lepton flavour violating (CLFV) processes such as $\mu \to e\gamma$ are technically allowed through loop diagrams involving virtual neutrinos and a W boson, as it will be explained in more detail later on. However, the GIM mechanism induces an extreme suppression of the branching ratio. The contribution is therefore proportional to the mass differences between neutrino mass eigenstates, denoted as Δm^2_ν. In addition, the loop is suppressed by the scale of the weak interaction, appearing through the mass of the W boson.
This leads to a branching ratio that scales the following way:

$$\mathcal{B}(\mu \to e\gamma) \propto \left(\frac{\Delta m^2_\nu}{m^2_W}\right)^2$$

Given that the neutrino mass-squared differences are of the order $\Delta m^2_\nu \sim 10^{-5}$ eV^2, and the W boson mass is approximately $m_W \sim 80$ GeV, the predicted branching ratio becomes:

$$\mathcal{B}(\mu \to e\gamma) \sim 10^{-54}$$

This is many orders of magnitude below the range of values for which the current experimental resources are sensitive enough to measure. Therefore, any signal of CLFV would constitute clear evidence for physics beyond the Standard Model. [8, 21].

2.4 Charged Lepton Flavour Violation and New Physics

Given the extreme suppression in the SM, CLFV is actually one of the cleanest and most powerful ways to search for New Physics (NP). This has motivated theorists to explore several NP models that could allow observable CLFV. For instance, in supersymmetric (SUSY) theories, the slepton mass matrices (the sleptons are the SUSY partners of leptons) may not be diagonal in the same basis as the leptons themselves. This misalignment would allow CLFV at the one-loop level, with branching ratios even as high as 10^{-8} depending on the SUSY scale and flavour structure [22].

It is also worth to mention another way to study CLFV is in models with leptoquarks, hypothetical bosons that couple directly to a lepton and a quark at the same time. These particles appear in various theories beyond the Standard model, since leptoquarks can mediate CLFV decays such as $b \to s\mu\tau$ or $b \to se\mu$ at tree level, bypassing the GIM suppression entirely [14]. The presence of both flavour violation and a coupling to heavy quarks makes b decays considerably sensitive to leptoquark contributions.

2.5 CLFV in the $b \to s\ell^+\ell^-$ transition

An interesting place to look for CLFV is in $b \to s\ell^+\ell^-$ transitions. These are flavour-changing neutral currents (FCNCs), which are forbidden at tree level in the SM and only occur through loop processes, such as penguin and box diagrams. This makes them very rare, and thus are used widely in New Physics searches.

In fact, LHCb and other experiments have already found some anomalies in these transitions, even when both leptons have the same flavour, like for example $\mu^+\mu^-$. These results have triggered a wave of theoretical activity, suggesting that NP might be present and affecting lepton flavour differently [18].

For $b \to s\ell^+\ell^-$ decays, the GIM mechanism applies because of the fact that the quark flavour changes but the charge remains constant, since for both quarks, charge is equal to $C = -1/3e$ [23]. Because of FCNC, this process can only be described in a loop, since the Standard Model forbids FCNC at tree level, and only in loops is where Z bosons, which have a neutral charge, can couple b and s quarks. Another option to make this process possible would be a loop involving two W bosons in order to conserve the fact that the charge remains neutral.

This can be seen in the following diagram in Figure 1, where three different possibilities for the $b \to s\ell^+\ell^-$ decays are shown. In the left diagram, b decays into either a t, c or u quark and emits a W boson. This virtual positively charged quark emits a Z boson or a photon which then decays into the two leptons, and lastly the positively charged quark interacts again with the W boson to produce the s quark. In the diagram positioned in the middle, the process is similar, but in this case is the W boson the one that emits the a Z boson or photon that, as explained before, decays into the two leptons. Lastly, in the diagram on the right of Figure 1, it is possible to count with two W bosons, having an anti-neutrino coupling the two bosons and making them possible to decay into the two leptons, however this process would be the least probable among the three of them because of the complexity and the number of particles involved.

2.6 Λ_b^0 LFV decay

So far, the searches for CLFV have mainly focused on B mesons. For example, the LHCb collaboration has searched for $B^0 \to K^{*0}\tau^\pm\mu^\mp$ [18], setting upper limits on the branching ratio at the 10^{-5} level. However, less attention has been paid to baryonic decays, such as the case of Λ_b^0. These are also

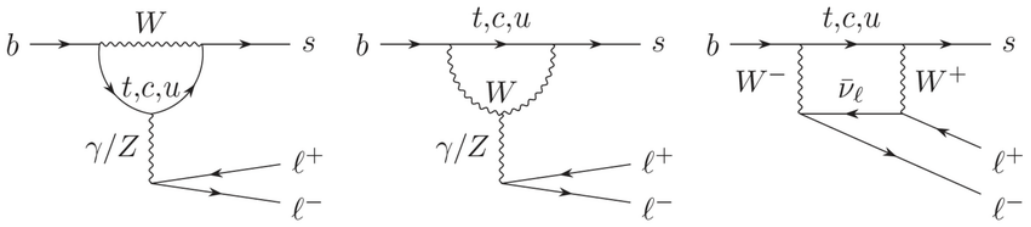

Figure 1: Diagrams for $b \to s\ell^+\ell^-$ decays [24].

sensitive to the $b \to s$ transition, but the kinematics and backgrounds are different from the mesonic decays, potentially offering complementary information.

The Λ_b^0 baryon has a quark content of *udb*, and it can decay into a Λ^0 (*uds*) plus two charged leptons [19]. The mass of this baryon is $m_{\Lambda_b^0} = 5.61960$ GeV [1]. If those leptons have different flavours, like a muon and a tau, it is safe to assume that LFV clearly takes place, since the initial state lacks of any type of leptons. The mean lifetime of the Λ_b^0 baryon is 1.470 ± 0.010 ps [19]. It decays via the weak interaction, which allows flavour-changing neutral current transitions such as $b \to s\ell^+\ell^-$. In this decay, the Λ_b^0 transitions into a Λ^0 baryon, which is formed by an up, a down, and a strange quark (*uds*). The Λ^0 has a mass of 1.115683 GeV and a relatively long lifetime of 2.63210^{-10} s [19], making it experimentally distinguishable thanks to its displaced decay vertex.

The leptons present in the final state also exhibit distinct characteristics. The muon μ, with a mass of 0.105658 GeV and a lifetime of 2.19710^{-6} s, is a stable and well-identified particle in collider experiments. On the other hand, the tau lepton τ, which has a much larger mass of 1.77686 GeV and a shorter lifetime of 2.90310^{-13} s, decays promptly, often into multiple final-state particles including hadrons or lighter leptons [25]. These differences in mass and lifetime between the muon and tau have a direct impact on the kinematical reconstruction of the decay. In particular, the prompt decay of the τ results in missing energy due to undetected neutrinos, complicating full mass reconstruction. Meanwhile, the relatively long-lived Λ^0 leaves a measurable decay vertex, allowing more accurate vertex fitting and particle identification. These properties must be considered both at the simulation level and during the application of selection cuts, in order to discriminate signal from background and improve reconstruction efficiency.

Knowing that Λ^0 decays into a proton and a negative pion, the reconstruction is feasible in experiments like LHCb, where displaced vertices and excellent tracking resolution make this analysis possible. The muon lepton can be considered to stay in its state and not decaying to another particles, while the tau lepton is considered to decay into three pions and a tau neutrino, conserving the lepton number in this secondary decay [26].

Background processes must count with the same daughter particles as the $\Lambda_b^0 \to \Lambda^0\mu^\pm\tau^\mp$ decay. The option is the $\Lambda_b^0 \to \Lambda^0\tau^\pm\tau^\mp$ decay, which conserves the lepton flavour number and where one of the tau leptons, with the same charge as the tau lepton from the signal decay, also decays into three pions and a tau neutrino, and where the other tau lepton decays into a muon of the same charge and two neutrinos: a tau neutrino and a muon neutrino. Because of the fact that this decay has to conserve the lepton flavour number, there must be a muon anti-neutrino if the muon is negatively charged and a muon neutrino if the muon is positively charged. The tau neutrino must have the same sign as the tau from the initial state of this subdecay.

Hence, by analyzing the kinematics of simulated $\Lambda_b^0 \to \Lambda^0\mu^\mp\tau^\pm$ decays and comparing them to background processes, it is possible to assess the feasibility of detecting CLFV in this mode. This type

[1] For this research, the units for mass will be in GeV, using c=1.

of research is important in order to extend the knowledge that there is nowadays about the Standard Model and Subatomic Physics, and the findings of this research can provide clues to amplify the understanding of this crucial field in Physics.

3 Experimental Setup

The experimental context of this research is based on the LHCb detector, located at the Large Hadron Collider (LHC) at CERN. LHCb is specifically designed for precision studies of b- and c-hadron decays, and it is optimally suited for detecting particles in the forward direction, covering a pseudorapidity range of $2 < \eta < 5$ [27]. The detector is composed of subcomponents, each of them contributing to a precise reconstruction of the kinematic properties of particles produced in proton-proton collisions. The closest to the interaction point is the Vertex Locator (VELO), which allows for an exceptionally accurate reconstruction of the primary and secondary vertices. This is crucial for identifying the decay of long-lived hadrons such as the Λ_b^0.

Particle identification is achieved through two Ring Imaging Cherenkov (RICH) detectors, which allow the experiment to distinguish between charged hadrons like pions, kaons, and protons across a broad momentum range. This capability is key to suppressing backgrounds and identifying final state particles in decays such as $\Lambda_b^0 \to \Lambda^0 \mu^{\mp} \tau^{\pm}$. Further downstream, the calorimeter system consists of an Electromagnetic Calorimeter (ECAL) and a Hadronic Calorimeter (HCAL), which measure the energy of electrons, photons, and hadrons. These calorimeters also contribute to the online event selection process. At the very end of the detector, the muon chambers are used in order to tag muons, which penetrate deeply due to their minimal interaction with matter. These detectors, interleaved with iron absorbers, are essential for identifying the muon in the signal decay. Figure 2 illustrates a side view of the LHCb detector and the layout of its major components.

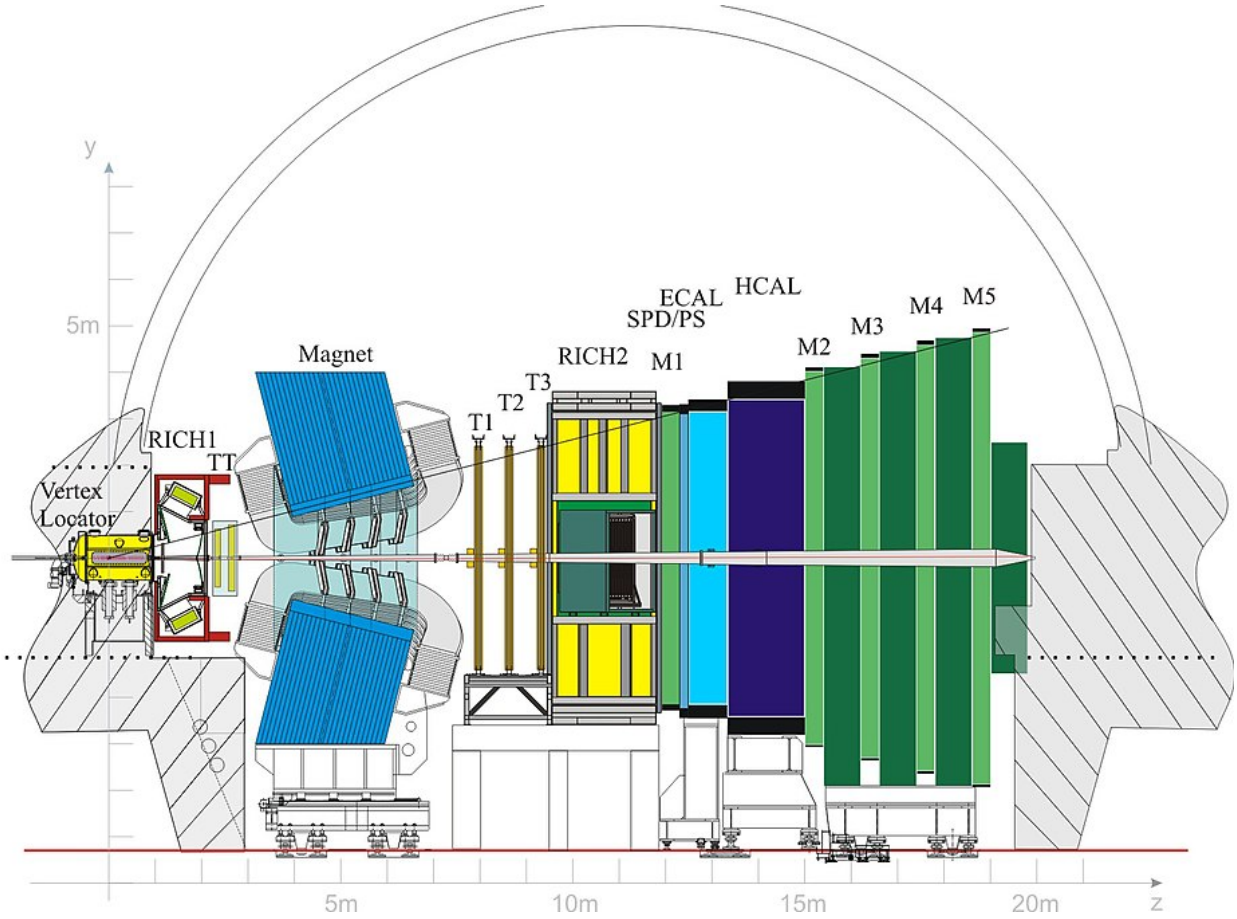

Figure 2: Schematic side view of the LHCb detector [28].

An important feature of the experimental context is the Run 3 upgrade, which introduces a full software-based trigger system that replaces the previous hardware-level trigger. This software trigger allows for event selection using full event reconstruction directly after data acquisition, improving the efficiency for selecting rare or complex decay signatures. Such a system is particularly advantageous for studies like this one, where lepton flavour violating decays involve final states with multiple tracks and displaced vertices [29].

Although this feasibility study is based on Monte Carlo data generated with the fast simulation tool RapidSim [30], rather than the full LHCb simulation framework, the generated events reproduce realistic kinematic distributions and detector resolutions expected at LHCb. RapidSim is a lightweight simulation tool developed specifically for fast generation of heavy-flavour decays, allowing for efficient testing of signal hypotheses with simplified detector effects and configurable resolution smearing, which means that realistic measurement uncertainties are introduced to the simulation in order to obtain reliable results [30].

The signal decay studied in this work is $\Lambda_b^0 \to \Lambda^0 \mu^\pm \tau^\mp$, where the Λ^0 subsequently decays to $p\pi^-$ and the τ lepton is assumed to decay into hadrons via $\tau^\mp \to \pi^\mp\pi^\mp\pi^\pm\nu_\tau$. This leads to a visible final state composed of a proton, three charged pions, and a muon, while the neutrino escapes detection. The topology is therefore characterized by multiple displaced vertices and missing energy, which adds complexity to the reconstruction.

4 Methods

The decay channel under study is $\Lambda_b^0 \to \Lambda^0 \mu^- \tau^+$, with the τ^+ lepton decaying into $\pi^+\pi^-\pi^+\overline{\nu_\tau}$ and the Λ^0 baryon decaying into $p^+\pi^-$. The alternative charge combination $\Lambda_b^0 \to \Lambda^0 \mu^+ \tau^-$, with the τ^- lepton decaying into $\pi^-\pi^+\pi^-\overline{\nu_\tau}$ has also been studied, nevertheless only the results for the first charge combination will be shown. In addition to that, the decays for $\overline{\Lambda_b^0}$ will be left out in order to maintain the report concise, since no differences are expected in the simulation setup. Both the simulated signal and background samples were generated using RapidSim. As only the charge combination mentioned in the beginning will be considered, the background process taken into consideration for this research is $\Lambda_b^0 \to \Lambda^0 \tau^- \tau^+$ where the τ^+ lepton decays into $\pi^+\pi^-\pi^+\bar{\nu}_\tau$ and the τ^- decays into $\mu^-\nu_\tau\overline{\nu_\mu}$

4.1 RapidSim

To study the feasibility of the lepton flavour violating decay channel $\Lambda_b^0 \to \Lambda^0 \mu^\mp \tau^\pm$, Monte Carlo signal events were generated using the fast simulation tool RapidSim [30]. This framework allows the user to efficiently simulate heavy-flavour hadron decays while incorporating key detector effects, such as momentum smearing and geometric acceptance, based on user-defined configurations.

A custom decay file was written to describe the full signal topology, including the decay of the tau lepton through a hadronic mode. Specifically, the following decay chain was defined: $\Lambda_b^0 \to \Lambda^0 \mu^- \tau^+$ with the tau subsequently decaying via $\tau^+ \to \pi^+\pi^-\pi^+\bar{\nu}_\tau$ This configuration reflects the realistic final-state particles expected in such events, capturing the displaced vertices and missing energy due to the undetected neutrino.

The simulation was performed in the LHCb Run 2 kinematic configuration, setting a beam energy of 6500 GeV per proton and selecting the appropriate angular acceptance of the LHCb detector ($2 < \eta < 5$, being η the pseudorapidity, which describes the angle of a particle relative to the beam). Detector smearing was applied to the momenta of all final-state particles using RapidSim predefined LHCb resolution settings. This smearing simulates the effects of momentum resolution limitations in the tracking system and is crucial to mimic real detector behavior.

In total, 10,000 events were generated using this configuration for each decay. These events were stored in ROOT format and subsequently analyzed using Python and ROOT-based tools. Distributions such as invariant mass and corrected mass were extracted, and selection cuts were applied to identify potential signal-like candidates. Although RapidSim does not perform full detector simulation or include background processes, it provides fast and accurate access to the kinematic phase space of rare decays, making it a valuable tool for feasibility studies such as this.

4.2 Parameters

To isolate the signal from the background, kinematic variables were explored. The most relevant among them are the invariant mass m_{inv} of the visible decay products and the corrected mass m_{corr}, defined respectively by the following equations:

$$m_{inv} = \sqrt{\left(\sum E_i\right)^2 - \left(\sum \vec{p}_i\right)^2}, \tag{1}$$

$$m_{corr} = \sqrt{m^2 + p_T^2} + p_T. \tag{2}$$

Here, m_{inv} represents the invariant mass of the visible decay products, while p_T is the transverse momentum of the reconstructed system relative to the flight direction of the Λ_b^0 baryon. These vari-

ables are essential when dealing with decay channels that include invisible final-state particles, such as neutrinos, which escape detection and carry away unknown amounts of energy and momentum. In such partially reconstructed decays, like $\Lambda_b^0 \to \Lambda^0 \mu^{\mp} \tau^{\pm}$, where the τ lepton subsequently decays into visible particles and a neutrino, the invariant mass alone underestimates the parent particle mass because it does not account for the missing energy.

To address this, the corrected mass variable is introduced, and it is defined using equation 2.

This expression effectively provides a lower-bound estimate of the true mass of the parent particle, incorporating both the visible invariant mass and an estimate of the missing transverse energy carried by undetected particles. The corrected mass improves mass resolution in decays involving neutrinos, enhancing the ability to discriminate signal from background. Its use is therefore crucial in feasibility studies of lepton flavour violating processes involving τ leptons.

4.3 Cuts

To ensure realistic and clean signal candidates, several selection criteria referred to as cuts were applied to the simulated datasets. These are designed to reject background processes while retaining as much of the signal as possible. The selection cuts follow standard procedures adopted in LHCb searches for similar decay channels, provided by the research team.
The signal decay $\Lambda_b^0 \to \Lambda^0 \mu^- \tau^+$ involves three primary final state components: the Λ^0 baryon and the tau lepton decaying into hadrons, and the oppositely charged muon. In specific, Λ^0 decays to a proton and a negative pion, whilst τ^+ decays to two positive pions, one negative pion and a tau anti-neutrino. Each of these components is reconstructed and filtered through a series of requirements. A schematic of this decay can be seen in Figure 3.

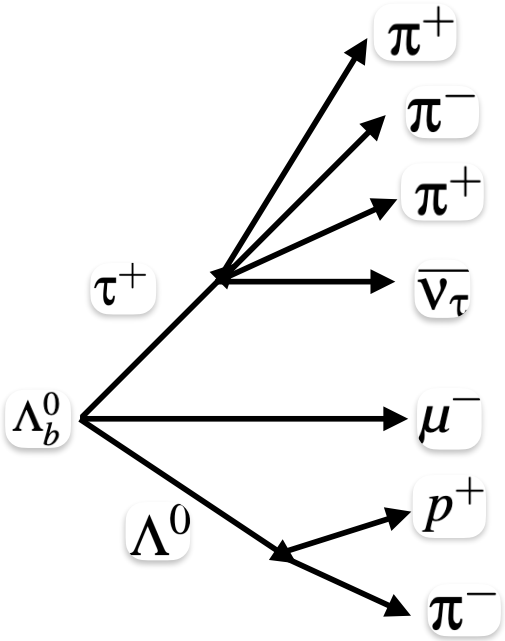

Figure 3: Decay diagram of $\Lambda_b^0 \to \Lambda^0 \mu^- \tau^+$ and the respective sub-decays.

The Λ^0 is reconstructed through its dominant decay mode $\Lambda^0 \to p\pi^-$. The proton and pion candidates are selected based on their momentum and particle identification PID information. The Λ^0 vertex is required to be well displaced from the primary vertex, with good vertex fit quality and a reconstructed invariant mass within a narrow window around the known Λ^0 mass $m_{\Lambda^0} = 1.115$ GeV. This helps to reduce combinatorial background and ensures that only long-lived baryons consistent with a Λ^0 hypothesis are selected.

Tau candidates are required to decay into hadrons, reconstructed from combinations of charged pions that satisfy several kinematic and geometric criteria. Each pion is required to have a transverse momentum p_T greater than 250 MeV and a total momentum p above 2 GeV. To ensure good vertex reconstruction, the impact parameter χ^2 IPχ^2 of the pions with respect to the primary vertex had to exceed 16. The most energetic pion in the decay was required to have $p_T > 800$ MeV and IP$\chi^2 > 25$.

Leptons were selected depending on whether a muon or electron was used in the signal. Muons were required to have $p > 3$ GeV, $p_T > 500$ MeV, and satisfy PID$_\mu > 2$ and ISMUON = True. The particle identification (PID) variables are numerical values assigned to each reconstructed particle candidate, reflecting the likelihood of that particle being a specific type, derived from information collected by the Ring Imaging Cherenkov (RICH) detectors, calorimeters, and muon stations. The `ISMUON` flag is a binary criterion indicating whether a track has left hits in the muon chambers consistent with a minimum ionizing particle, as expected for a muon. This flag is essential for distinguishing genuine muons from hadrons that may punch through the detector layers. In the selection cuts, requiring `ISMUON` ensures high muon purity.

Tau pairs were combined to form candidate signal decays if their invariant mass was within 200 MeV to 5 GeV and passed a separation requirement on vertex significance.

Finally, the full lambda beauty baryon candidate Λ_b^0 was constructed by combining these tau pairs and taking into consideration the mass $m_{\Lambda_b^0} = 5.61960$ GeV. Additional criteria were imposed on the flight direction (with $\cos\theta > 0.995$), transverse displacement from the primary vertex (> 0.3 mm) and an impact parameter χ^2 (< 40). The angle θ is defined as the angle between the reconstructed momentum vector of a particle and the vector pointing from the primary vertex to the decay vertex. The variable χ^2 refers to the impact parameter chi-squared, which quantifies how significantly a track is displaced from the primary vertex.

5 Results

After simulating the decays, different distributions were achieved as results.

The distribution for the invariant mass of the signal decay $\Lambda_b^0 \to \Lambda^0 \mu^- \tau^+$ with the cuts applied is shown in Figure 4.

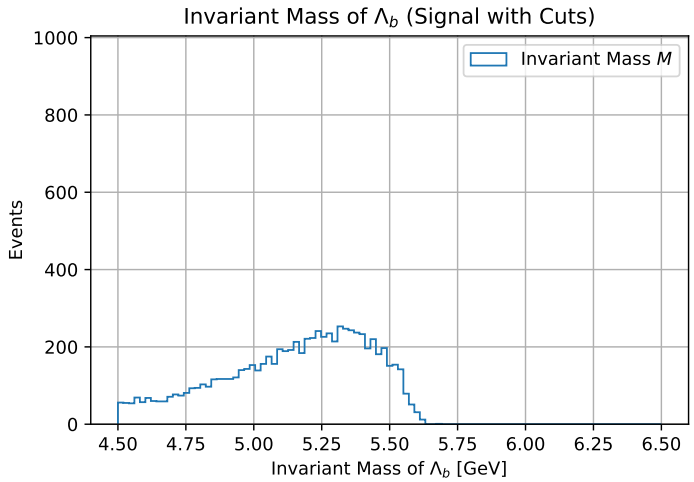

Figure 4: Invariant mass of Λ_b^0 candidates from simulated $\Lambda_b^0 \to \Lambda^0 \mu^- \tau^+$ events in GeV.

The invariant mass of Λ_b^0 is shown with a maximum between the range of 5.25 GeV and 5.50 GeV, which is very near to the actual mass of Λ_b^0 which is $m_{\Lambda_b^0} = 5.61960$ GeV [19]. The distribution shows a tail in the left region of the axis, which means events with lower mass values. At the right part of the distribution, the number of events decreases until detecting none of them for values higher than 5.75 GeV.

This shape of the invariant mass distribution can be attributed to the presence of undetected neutrinos in the final state. Since neutrinos do not leave signals in the detector, their momenta are not reconstructed, leading to an underestimate of the total invariant mass for some events. This results in a broader distribution toward lower mass values.

Now, this distribution of the invariant mass of Λ_b^0 is compared to the distribution of the corrected mass of Λ_b^0, as well as the current most precise measured value of the Λ_b^0 baryon [19], as seen in Figure 5.

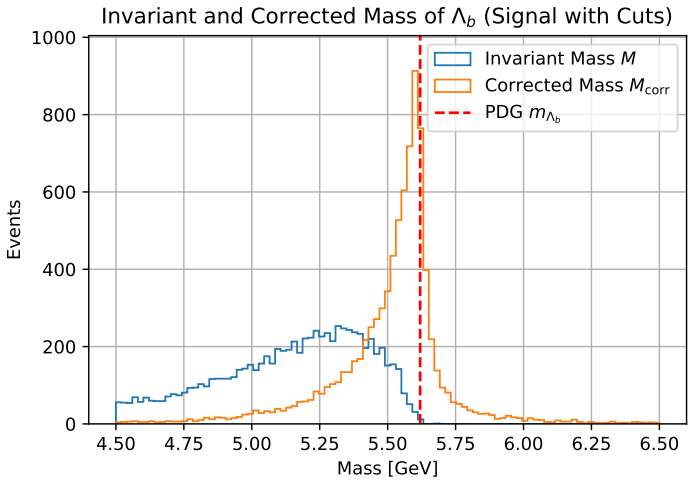

Figure 5: Invariant mass and corrected mass of Λ_b^0 in GeV, including the current most precise measured value of the Λ_b^0 baryon in GeV [19].

As it can be seen in Figure 5, the distribution of the corrected mass of Λ_b^0 is more precise and noticeably sharper than the distribution of the invariant mass. This is because the corrected mass accounts for the missing transverse momentum, helping to partially compensate for the presence of undetected neutrinos in the decay. In addition to that, the peak of the distribution that represents the corrected mass is displaced to the right with respect to the distribution of the invariant mass of Λ_b^0. This also makes sense, since the invariant mass underestimates the true mass of the parent particle when invisible particles like neutrinos are present. The corrected mass, by including transverse momentum, shifts the distribution closer to the true value. Furthermore, the maximum is very near to the current most precise measured value of the Λ_b^0 baryon mass value which is equal to 5.61960 GeV.

Between the invariant mass and the corrected mass, shown their distributions together in Figure 5, the latter is better suited for the search of LFV Λ_b^0 decays. This is because it partially recovers the mass of the parent particle even in the presence of invisible final state particles like neutrinos. As a result, it produces a sharper and more accurately centered peak, improving the signal resolution and making it easier to distinguish from background. The two distributions are already very distinguishable one from another, being the invariant mass distribution very undefined in comparison to the precise shape that the corrected mass distribution has.

Moreover, more variables were checked in the process of finding the variable more suitable for the search of LFV Λ_b^0 decays, attached in the Appendix A.

After obtaining the distributions for the invariant mass and the corrected mass of the signal decay, next the signal is compared to the potential background process in order to look for differences between them, as a function of different parameters.

In Figure 6 is shown the distribution of the invariant mass for both the signal and the background after the cuts are applied.

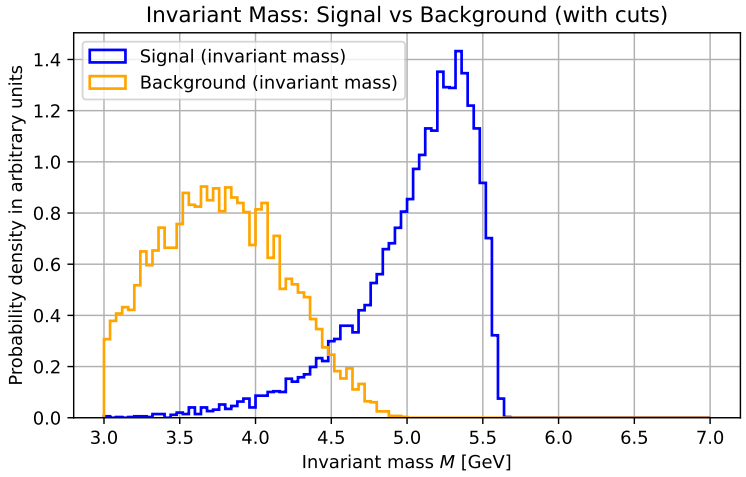

Figure 6: Invariant mass of Λ_b^0 baryon for signal decay and background decay in GeV.

It is clearly noticeable from Figure 6 how different the signal is from the background. The signal distribution has a maximum between the values of 5.0 GeV and 5.5 GeV. This outcome is already explained after Figure 4. On the other hand, the background distribution is displaced to the left with respect to the signal distribution, being a very broad distribution with the highest probability density between the values of 3.5 GeV and 4.0 GeV. The reason why the invariant mass of the background process looks clearly distinguishable from the signal is explained because of the fact that the background process counts with three neutrinos in its final state, one from the positive tau lepton sub-decay and two from the negative tau lepton sub-decay. That means that the final state of the background process counts with two more neutrinos in comparison with the final state of the signal process. Knowing that neutrinos are massless and undetectable, the momenta that corresponding to the neutrinos is only reconstructed when the corrected mass is calculated. That missing momenta that is only taken into account in the corrected mass and not in the invariant mass must be higher for a final state with three neutrinos rather than for a final state with only one neutrino. Thus, the difference between the distributions is explained.

Furthermore, the distributions of the corrected mass for both the signal decay and the background decay are represented in Figure 7.

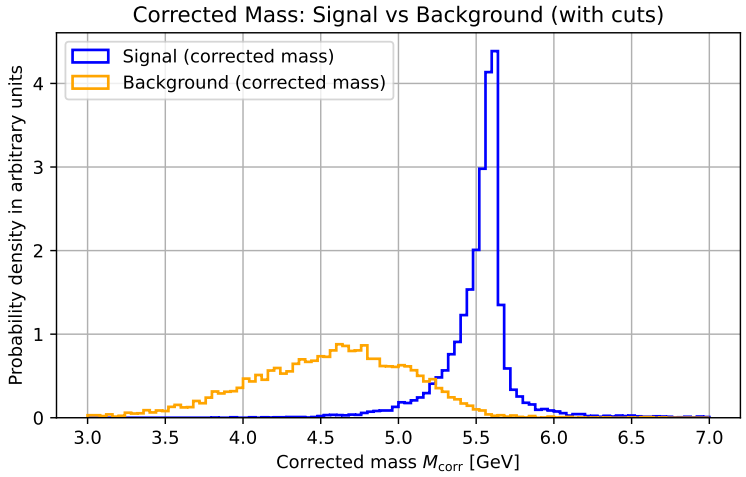

Figure 7: Corrected mass of Λ_b^0 baryon for signal decay and background decay in GeV.

In Figure 7, the signal distribution is a very sharp maximum near the value of Λ_b^0 whilst the background distribution is a small and broad shape. The background is also considerably displaced to the left with respect to the signal distribution, with the probability density being higher between the values of 4.5 GeV and 5.0 GeV. The reason the background distribution looks the way is represented arises because of the smearing considered after calculating the corrected mass for both the signal and the decay. The background decay has three neutrinos in its final state whilst the signal decay has only one neutrino in its final state. Thus, when the corrected mass is calculated for both cases, the uncertainty of the background process is higher than the uncertainty of the signal process, leading to a very broad distribution and not as sharp as the signal decay distribution.

Both the invariant mass and the corrected mass are very suitable in order to distinguish the signal process from the potential background process. As it has been commented before, the presence of more neutrinos in the final state of the background process than in the final state of the signal process leads to the invariant mass of the background process being much lower than the invariant mass of the signal process. Due to the same reason, it leads to the corrected mass of the background process being lower and also more uncertain than the corrected mass of the signal process. Between the two, Figure 7 displays the highest discrepancy between signal and backgrounds, since the background distribution is much broader than the signal distribution, making them even more distinguishable than in Figure 6.

6 Discussion

The results presented in the previous section demonstrate that the corrected mass variable provides a sharper and more accurate representation of the Λ_b^0 baryon mass than the invariant mass. This is particularly important for decays with invisible final state particles such as neutrinos, where significant momentum is lost. The corrected mass compensates partially for this, improving the resolution of the signal peak and making it more distinguishable from background. This has been proved by analysing Figures 5 and 7.

The clear separation between the signal and background distributions, especially in the corrected mass as it is visible in Figure 7, highlights the potential of this observable for distinguishing lepton flavour violating (LFV) Λ_b^0 decays from dominant Standard Model backgrounds.

In order to address the research questions, it is safe to state the following: due to the fact that the corrected mass is the most suitable parameter to both obtain a more precise value for the Λ_b^0 baryon mass and is also the most useful parameter to distinguish signal from background, it is therefore feasible to search for LFV Λ_b^0 decays. This LFV decay $\Lambda_b^0 \to \Lambda^0 \mu^- \tau^+$ can be differentiated from the potential background decay $\Lambda_b^0 \to \Lambda^0 \tau^- \tau^+$ because of the fact that the three neutrinos present in the final state of the background decay signify a higher loss in energy and therefore higher uncertainty in its distributions than the neutrino present in the final state of the signal decay.

However, there are limitations inherent to this study. The use of RapidSim means the simulation lacks a full detector model, and smearing was applied manually rather than obtained from real detector responses. This affects the realism of the distributions, especially for background processes with multiple neutrinos. Additionally, no efficiencies or systematic uncertainties have been estimated at this stage.

In future work, the use of full Monte Carlo simulations from the LHCb framework would improve the accuracy of the distributions, especially for background. It would also enable more reliable estimation of efficiencies, acceptances, and systematic uncertainties. Furthermore, it would enable a more detailed multivariate analysis and optimization of selection cuts.

Moreover, factoring in more potential background processes is useful to increase the level of reliability of the results. Background processes are unavoidable, since it is something inherent in the nature of Physics processes. When considering one of the possible decay channels as the signal decays, it is essential to considerate that other decay channels will happen simultaneously since they have a certain probability. These other decay channels different from the signal are background processes, and if they are all considered, it would be a more realistic approach in order to discriminate the signal among the background processes. For this study, only one potential background process was considered, but including more would give more promising results.

To keep finding about lepton flavour violation, it is of high interest to do researches as this one for other LFV decays, such as $B \to \pi \mu^{\pm} \tau^{\mp}$ or $D \to K \mu^{\pm} \tau^{\mp}$ decays with potential background processes happening for each of them. Carrying out a research like this would shed a light on Physics Beyond the Standard Model.

7 Conclusion

In this research project, a feasibility study was conducted to assess whether the lepton-flavour violating decay $\Lambda_b^0 \to \Lambda^0 \mu^- \tau^+$ can be effectively distinguished from Standard Model background processes using simulated data. In essence, this study aimed to known which were the variables that provided the most discrepancies between the distributions, in order to identify the signal from the potential background.

The analysis showed that the corrected mass significantly improves the resolution of the reconstructed Λ_b^0 mass when compared to the invariant mass. This improvement is particularly important for decays involving undetected neutrinos, where the corrected mass recovers part of the lost momentum and provides a distribution that peaks close to the true mass of the parent particle.

Furthermore, the comparison between signal and background demonstrated that the corrected mass distribution for signal events is shown as sharp and placed near the current measured value for Λ_b^0, whereas the background—dominated by decays involving three neutrinos—shows a broader and left-shifted distribution. This clear distinction enhances the potential of the corrected mass to discriminate signal from background and supports the viability of pursuing this decay channel as an evidence of LFV at LHCb.

However, the study also revealed limitations, primarily due to the use of RapidSim, which lacks a full detector simulation. Smearing effects were applied manually, and systematic uncertainties and selection efficiencies were not included. Therefore, while the trends observed are promising, the conclusions drawn remain qualitative.

Future work should incorporate full Monte Carlo simulations within the LHCb software framework to evaluate efficiencies, systematics, and real detector effects more accurately. Moreover, extending the analysis to include multivariate techniques or additional discriminating variables could further enhance the sensitivity of the search.

Despite current limitations, a step has been made in the search of Physics Beyond the Standard Model, achieving a very small piece of the whole puzzle that describes the mystery of the Universe.

Bibliography

[1] D. J. Gross, *The role of symmetry in fundamental physics*, Proceedings of the National Academy of Sciences **93** (1996) 14256, arXiv:https://www.pnas.org/doi/pdf/10.1073/pnas.93.25.14256.

[2] R. Lehnert, *CPT symmetry and its violation*, Symmetry **8** (2016) 114.

[3] S. F. Novaes, *Standard model: An introduction*, 2000.

[4] LHCb Collaboration, *Observation of a new particle in the search for the standard model higgs boson with the atlas detector at the lhc*, Physics Letters B **716** (2012) 1–29.

[5] S. M. Bilenky, *Neutrino masses, mixing, and oscillations*, Nuclear Physics B - Proceedings Supplements **265-266** (2016) 161.

[6] P. Langacker, *The standard model and beyond*, CRC Press (2009), ISBN: 978-1-4200-8276-8.

[7] S. L. Glashow, J. Iliopoulos, and L. Maiani, *Weak interactions with lepton–hadron symmetry*, Physical Review D **2** (1970) 1285–1292.

[8] S. T. Petcov, *The processes $\mu \to e\gamma$, $\mu \to ee\bar{e}$, neutrino oscillations and leptonic CP violation*, Soviet Journal of Nuclear Physics **25** (1977) 340.

[9] R. H. Bernstein and P. S. Cooper, *Charged lepton flavor violation: An experimenter's guide*, Physics Reports **532** (2013) 27.

[10] J. Heeck, *Interpretation of lepton flavor violation*, Physical Review D **95** (2017) .

[11] T. Kajita, *Nobel lecture: Discovery of atmospheric neutrino oscillations*, Rev. Mod. Phys. **88** (2016) 030501.

[12] J. Zupan, *Introduction to flavour physics*, 2019.

[13] M. Aoki *et al.*, *Charged lepton flavour violations searches with muons: present and future*, 2025.

[14] A. Crivellin, S. Najjari, and J. Rosiek, *Lepton flavor violation in the standard model with general dimension-six operators*, Journal of High Energy Physics **2014** (2014) .

[15] M. Ardu and G. Pezzullo, *Introduction to charged lepton flavour violation*, arXiv preprint arXiv:2204. 08220 (2022).

[16] W. Altmannshofer, P. Stangl, and D. M. Straub, *Interpreting hints for lepton flavor universality violation*, Physical Review D **96** (2017) 055008.

[17] A. Greljo, G. Isidori, and D. Marzocca, *On the breaking of lepton flavor universality in b decays*, Journal of High Energy Physics **2015** (2015) 142.

[18] L. Collaboration, F. Polci *et al.*, *Search for the lepton-flavour violating decays $b^0 \to k^{*0}\tau^{\pm}\mu^{\mp}$*, Journal of High Energy Physics **2023** (2023) 143, arXiv:2209.09846, LHCb-PAPER-2022-021, CERN-EP-2022-154.

[19] Particle Data Group, S. Navas *et al.*, *Review of particle physics*, Phys. Rev. D **110** (2024) 030001.

[20] Z. Maki, M. Nakagawa, and S. Sakata, *Remarks on the unified model of elementary particles*, Progress of Theoretical Physics **28** (1962) 870–880.

[21] J. Heeck, *Interpretation of lepton flavor violation*, Physical Review D **95** (2017) 015022.

[22] R. Barbieri, L. J. Hall, and A. Strumia, *Violations of lepton flavour and CP in supersymmetric unified theories*, Nuclear Physics B **445** (1995) 219–251.

[23] S. N. et al. (Particle Data Group), *Review of particle physics*, Physical Review D **110** (2024) 030001, See "Quarks" summary tables, RPP2024, `rpp2024-sum-quarks.pdf`.

[24] S. Bahinipati, *Review of flavor anomalies*, Symmetry **15** (2023) 1963.

[25] M. T. et al. (Particle Data Group), *Review of particle physics*, Phys. Rev. D **98** (2018) 030001, See "Leptons" summary tables, RPP2019, `rpp2019-sum-leptons.pdf`.

[26] M. T. et al. (Particle Data Group), *Review of particle physics*, Physical Review D **98** (2018) 030001, See "Leptons" summary tables, RPP2019, `rpp2019-sum-leptons.pdf`.

[27] LHCb Collaboration, *The LHCb detector at the lhc*, JINST **3** (2008) S08005.

[28] LHCb Collaboration, *LHCb: Technical design report*, CERN-LHCC-2003-030, CERN, 2003. CERN-LHCC-2003-030.

[29] LHCb Collaboration, *LHCb trigger and online upgrade for run 3*, CERN-LHCC-2014-016, LHCb-TDR-016 (2014).

[30] G. A. Cowan, *RapidSim: an application for the fast simulation of heavy-quark hadron decays*, 2016.

Appendix

A Additional Diagrams

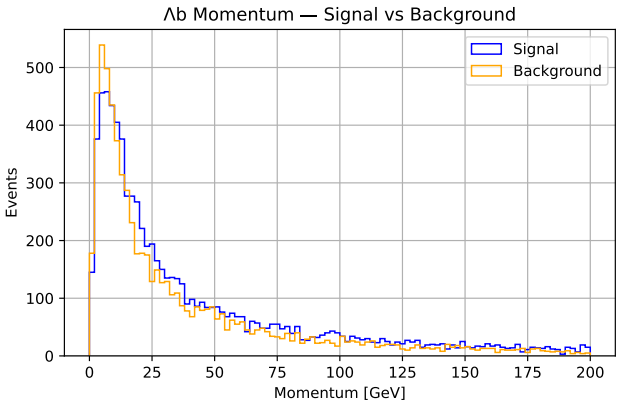

Figure 8: Momentum of Λ_b^0 baryon for signal decay and background decay in GeV.

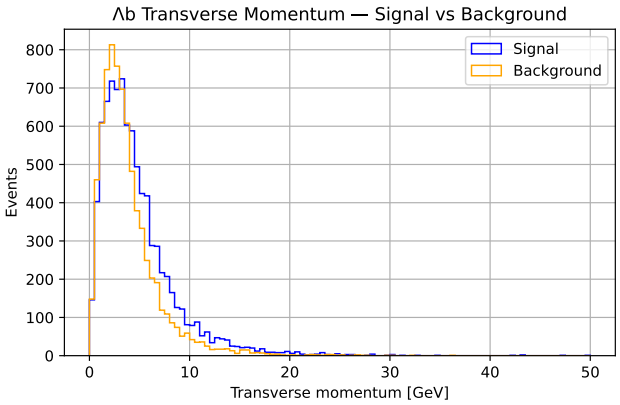

Figure 9: Transverse momentum of Λ_b^0 baryon for signal decay and background decay in GeV.

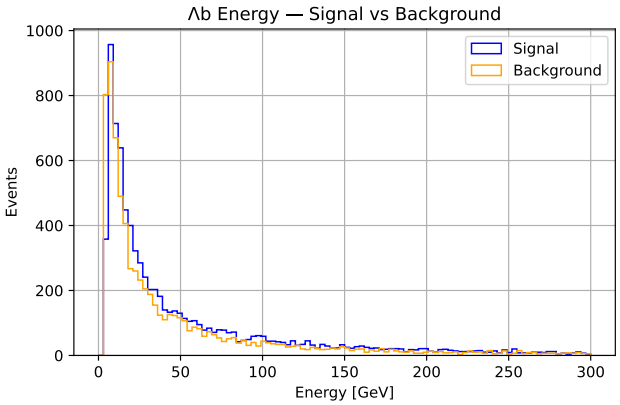

Figure 10: Energy of Λ_b^0 baryon for signal decay and background decay in GeV.

B RapidSim

Figure 11: Signal decay file of $\Lambda_b^0 \to \Lambda^0 \mu^- \tau^+$ in RapidSim.

```
Lambdab0 -> {Lambda0 -> p+ pi-} mu- {tau+ -> pi+ pi- pi+ anti-nutau}
```

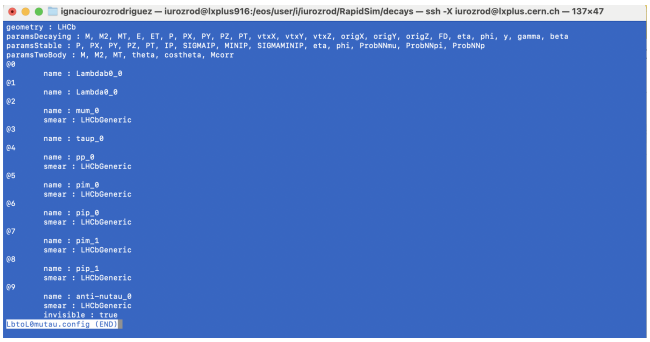

Figure 12: Signal configuration file of $\Lambda_b^0 \to \Lambda^0 \mu^- \tau^+$ in RapidSim.

```
geometry : LHCb
paramsDecaying : M, M2, MT, E, ET, P, PX, PY, PZ, PT, vtxX, vtxY, vtxZ,
   origX, origY, origZ, FD, eta, phi, y, gamma, beta
paramsStable : P, PX, PY, PZ, PT, IP, SIGMAIP, MINIP, SIGMAMINIP, eta,
   phi, ProbNNmu, ProbNNpi, ProbNNp
paramsTwoBody : M, M2, MT, theta, costheta, Mcorr

@0
  name : Lambdab0_0
@1
  name : Lambda0_0
@2
  name : mum_0
  smear : LHCbGeneric
@3
  name : taup_0
@4
  name : pp_0
  smear : LHCbGeneric
@5
  name : pim_0
  smear : LHCbGeneric
@6
  name : pip_0
  smear : LHCbGeneric
@7
```

```
  name : pim_1
  smear : LHCbGeneric
@8
  name : pip_1
  smear : LHCbGeneric
@9
  name : anti-nutau_0
  smear : LHCbGeneric
  invisible : true
```

Figure 13: Background decay file of $\Lambda_b^0 \to \Lambda^0 \tau^- \tau^+$ in RapidSim.

```
Lambdab0 -> {Lambda0 -> p+ pi-} {tau- -> mu- nutau anti-numu} {tau+ -> pi
   + pi- pi+ anti-nutau}
```

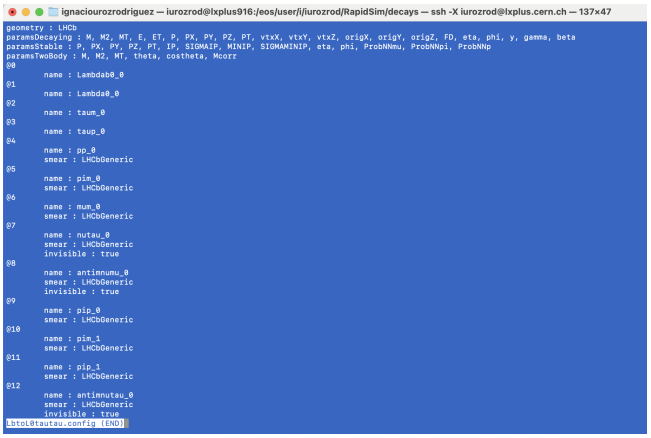

Figure 14: Background configuration file of $\Lambda_b^0 \to \Lambda^0 \tau^- \tau^+$ in RapidSim.

```
geometry : LHCb
paramsDecaying : M, M2, MT, E, ET, P, PX, PY, PZ, PT, vtxX, vtxY, vtxZ,
   origX, origY, origZ, FD, eta, phi, y, gamma, beta
paramsStable : P, PX, PY, PZ, PT, IP, SIGMAIP, MINIP, SIGMAMINIP, eta,
   phi, ProbNNmu, ProbNNpi, ProbNNp
paramsTwoBody : M, M2, MT, theta, costheta, Mcorr

@0
  name : Lambdab0_0
@1
  name : Lambda0_0
@2
  name : taum_0
@3
  name : taup_0
```

```
@4
  name : pp_0
  smear : LHCbGeneric
@5
  name : pim_0
  smear : LHCbGeneric
@6
  name : mum_0
  smear : LHCbGeneric
@7
  name : nutau_0
  smear : LHCbGeneric
  invisible : true
@8
  name : antinumu_0
  smear : LHCbGeneric
  invisible : true
@9
  name : pip_0
  smear : LHCbGeneric
@10
  name : pim_1
  smear : LHCbGeneric
@11
  name : pip_1
  smear : LHCbGeneric
@12
  name : antinutau_0
  smear : LHCbGeneric
  invisible : true
```